

# On the Effect of Fat Suppression via Chemically Selective Saturation (CHESS) Pulses on $R_2^*$ Measurements in Patients with Transfusional Iron Overload

Axel Joachim Krafft<sup>1</sup>, Ralf B. Loeffler<sup>1</sup>, Xiao Bian<sup>1,2</sup>, Ruitian Song<sup>1</sup>, Beth M. McCarville<sup>1</sup>, Jane S. Hankins<sup>3</sup>, and Claudia M. Hillenbrand<sup>1</sup>

<sup>1</sup>Radiological Sciences, St. Jude Children's Research Hospital, Memphis, TN, United States, <sup>2</sup>Rhodes College, Memphis, TN, United States, <sup>3</sup>Hematology, St. Jude Children's Research Hospital, Memphis, TN, United States

**TARGET AUDIENCE** Basic scientists and clinicians working on MRI based iron overload assessment

**PURPOSE** Hepatic fat (steatosis) is a major confounder in  $R_2^*$  based liver iron overload assessment [1] as fat-water modulations in the multi gradient echo (mGRE) signal eventually affect the  $T_2^*$  evaluation. Although various approaches such as IDEAL [2] or advanced data fitting [3] have been presented to simultaneously estimate  $T_2^*$  and fat-water content, the availability of these techniques remains limited. A simpler solution could be the inclusion of fat suppression (FS) techniques using chemically selective saturation (CHESS) pulses. However, decreasing  $T_2^*$  times as observed for increasing iron content correspond to broadened spectral profiles which overlap with the excitation band of the applied CHESS pulse. This partial saturation may alter the measured  $T_2^*$  times. This work investigates the effect of CHESS FS on the measured  $R_2^*$  values in 65 patients with transfusional iron overload and proposes a phenomenological model to explain and correct the observed changes.

## METHODS

**Theory:** The ideal, noise-free mGRE signal decay can be described as a mono-exponential function (decay rate:  $R_2^* = 1/T_2^*$ ,  $S_0$ : signal at  $t = 0$ ) which translates via Fourier transformation (FT) into a Lorentzian line shape in frequency domain  $f$  with a full width at half maximum (FWHM) that is directly related to  $R_2^*$ :

$$\text{FT}[S(t)] = \text{FT}\left[S_0 \cdot \exp(-R_2^* \cdot t)\right] = S_0 \cdot \frac{2 \cdot R_2^*}{R_2^{*2} + (2\pi \cdot f)^2} \quad \text{and} \quad \text{FWHM} = \frac{R_2^*}{\pi} \quad [1]$$

Figure 1 depicts the partial overlap between Lorentzian line profiles and a Gaussian CHESS FS pulse for different  $T_2^*$  times. As can be seen, the CHESS pulse influences spectral components of the water signal within its frequency spectrum which can be approximated as range of full saturation ('FS range') corresponding to the pulse bandwidth. In this simplified picture, spectral components within the FS range are removed from the detected signal ultimately resulting in a reduction of  $R_2^*$ . We account for this effect by calculating the change in the total area of the line profile ( $\Delta A_{FS}$ ).  $R_{2,FS}^*$ , the  $R_2^*$  value affected by the FS pulse, can then be obtained from the 'undisturbed'  $R_2^*$  value via:

$$R_{2,FS}^* = (1 - \Delta A_{FS}) \cdot R_2^* = \left(1 - \int_{f_{lo}}^{f_{hi}} \frac{2 \cdot R_2^*}{R_2^{*2} + (2\pi \cdot f)^2} df\right) \cdot R_2^* = \left(1 - \frac{1}{\pi} \arctan\left(\frac{2\pi \cdot f}{R_2^*}\right)\right)_{f_{lo}}^{f_{hi}} \cdot R_2^* \quad [2]$$

In Eq. 2,  $S_0$  represents a scaling factor and was set to 1. No further normalization is required as the integral of the Lorentzian equals to 1. The dashed line in Fig. 3 shows the theoretical  $R_{2,FS}^*$  values according to Eq. 2. Equation 2 cannot be solved analytically for  $R_2^*$ . However, based on the model a correction factor can be retrieved numerically for any  $R_2^* - R_{2,FS}^*$  pair and applied to correct the measured  $R_{2,FS}^*$  values and to attain undisturbed  $R_2^*$  values.

**MRI Patient Study and Analysis:** The effect of CHESS FS on  $R_2^*$  was evaluated in 66 liver data sets from 65 patients (42 female/23 male, mean age 19 years, range 4-46 years) enrolled in an ongoing IRB approved study to assess iron overload. All patients received multiple blood transfusions as part of their therapy (total # transfusions > 12). MRI scans were done at 1.5 T (Siemens Avanto) following the approach described in [4]. Each MRI exam included a single slice (SSL; TR/TE<sub>1</sub>/ΔTE = 200/1.1/0.8 ms, 20 echoes, matrix 128×104, thickness 10 mm), multi-slice (MSL; 11 interleaved slices, slice gap 10 mm, otherwise same parameters as SSL), and multi-slice with FS mGRE acquisition (5 interleaved slices, slice gap 10 mm, otherwise same parameters as SSL + Gaussian FS pulse: duration 10240 μs, center frequency 210 Hz, bandwidth 185 Hz). The SSL data was used as the reference data set to obtain the 'undisturbed'  $R_2^*$ , and the MSL sequence without FS was included to test if the application of additional excitation pulses for multi-slice imaging introduced an additional  $R_2^*$  bias from potential slice cross-talk.  $R_2^*$  maps were generated using non-linear least square fitting in MATLAB according to a quadratic signal model with noise correction [5]. For the MSL/FS data sets,  $R_2^*$  maps were calculated from the slice matching the location of the SSL acquisition. Whole liver ROIs were manually drawn and any unwanted structures, e.g. blood vessels, were excluded based on a histogram approach [6]. Mean  $R_2^*$  values were calculated from the remaining pixel values (Fig. 2).

**RESULTS & DISCUSSION** Figure 3 shows  $R_2^*$  results from SSL, MSL and FS mGRE acquisitions found in our patient group.  $R_2^*$  values from SSL and MSL images are in excellent agreement demonstrating that the multi-slice approach does not bias the  $R_2^*$  measurement. As expected from Eq. 2, FS  $R_2^*$  values are systematically smaller compared to the SSL results which would translate into an underestimation of the liver iron content based on the  $R_{2,FS}^*$  values (deviations about 10-15% for  $R_{2,FS}^* \geq 500$  1/s). Our model (Fig. 3, dashed line) is in good agreement with the measured data. Applying the model to the measured  $R_{2,FS}^*$  data yields corrected  $R_{2,FS}^*$  values that are very consistent with the SSL data. This indicates a successful removal of the FS induced bias. Further, this correction improves the accuracy of FS  $R_2^*$  measurements: the linear regression between SSL and corrected FS data exhibits a slope close to 1 and a y-intercept close to 0. In contrast to previous work [7], we found differences in  $R_2^*$  without and with CHESS FS. However in that study, measured  $T_2^*$  times were confined to a range  $\geq 3.5$  ms (i.e.  $R_2^* \leq 300$  1/s) where expected changes in  $R_2^*$  for non-FS and FS acquisitions are small according to our results (cf. Fig. 3). Although our simplified model does neither consider effects of signal noise nor relaxation effects during the FS pulse, which may be relevant for high  $R_2^*$  values, it consistently describes changes in  $R_2^*$  due to the application of CHESS FS pulses. The model is based solely on the physical properties of the CHESS pulse, i.e. center frequency and spectral bandwidth, and does not require additional input such as pulse sequence parameters. The model itself is not dependent on the employed  $T_2^*$  fitting approach; however, different  $T_2^*$  fitting approaches could alter the  $R_2^*$  quantification [5].

**CONCLUSION** We found that CHESS FS affects  $R_2^*$  and potentially biases iron overload assessment especially for high iron content. Our phenomenological model explains the observed changes and allows for a correction of the measured values. So far, all published liver biopsy calibrated  $R_2^*$ -MRI iron curves were derived from non-FS mGRE acquisitions. Hence, our findings are of clinical importance for  $R_2^*$  based iron overload assessment in scenarios where non-FS mGRE sequences are substituted with CHESS FS mGRE acquisitions, e.g. in patients with suspected steatosis.

**REFERENCES** [1] Wood JC et al. Blood 2005;106:1460-5. [2] Yu H et al. MRM 2008;60:1122-34. [3] Bydder M et al. MRI 2010;28:767-76. [4] Hankins JS et al. Blood 2009;113:4853-55. [5] Feng Y et al. MRM 2013;DOI:10.1002/mrm.24607. [6] McCarville BM et al. Pediatr Radiol 2010;40:1360-67. [7] Sanches-Rocha L et al. MRI 2013;DOI: 10.1016/j.mri.2013.07.013.

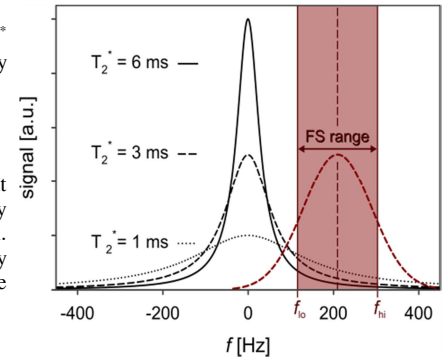


Fig. 1: Lorentzian line profiles for different  $T_2^*$  times and schematics of the Gaussian FS pulse (FS range indicates spectral saturation band).

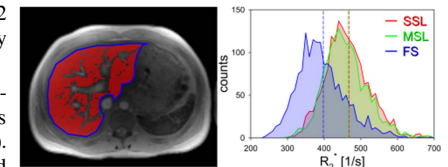


Fig. 2: Left: Example of whole liver ROI (blue) and area of included pixels (red overlay) after histogram analysis. Right: Distribution of  $R_2^*$  values for SSL, MSL and FS mGRE acquisitions. FS values are systematically smaller.

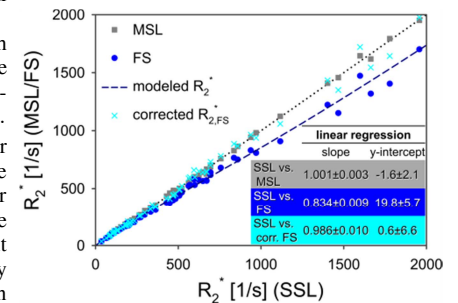


Fig. 3:  $R_2^*$  values found in 66 transfusional iron overload exams for SSL, MSL and FS mGRE acquisitions. The dashed line represents the  $R_{2,FS}^*$  values according to the model from Eq. 2.